Journal of Magnetism and Magnetic Materials 148 (1995) 226–231

ELSEVIER

Journal of magnetism and magnetic materials

Invited Paper

Magneto-optical domain studies in coupled magnetic multilayers

Rudolf Schäfer *

IFW, Helmholtzstraße 20, D-01069 Dresden, Germany

Abstract

Due to an information depth of at least 20 nm in metals, the direct study of the magnetization in several layers of a multilayer system is possible by magneto-optical microscopy. This is especially helpful for the investigation of coupled layers consisting of ferromagnetic films and non-magnetic spacer layers where according to oscillatory exchange coupling a different alignment of the magnetization in the neighboring films is possible. For such systems the combined use of the magneto-optical *Kerr, Voigt* and *gradient* effects proved very convenient. The potential of these effects is reviewed, together with an overview of domains in mono- and polycrystalline trilayers.

1. Introduction

Ferromagnetic thin films, interspaced by certain non-magnetic layers, are exchange coupled with an oscillation between ferromagnetic (F), antiferromagnetic (AF) [1], and — often observed in cubic materials — biquadratic coupling (90°) [2] as a function of interlayer thickness. Magneto-optics is applied in several ways to get information about the interaction of such layers: for instance, often the hysteresis curve is measured magneto-optically in order to identify the type and strength of coupling with a high lateral resolution. Another more recent method employs X-ray magnetic circular dichroism. This technique is element specific [3], allowing separate observations of the magnetizations in the different layers of a stack.

The present review, however, is devoted to direct imaging of the magnetic microstructure by magneto-optical *microscopy*. The method offers several advantages: no extra sample preparation is required, arbitrary magnetic fields can be applied and so the nucleation [2] and domain behavior responsible for the magnetization process can be studied in real time [4], and, most important, the magneto-optical information depth is at least 20 nm so that direct information about the magnetization in several layers within that thickness range can be obtained. Based on previous publications [2,5–7], we will summarize typical domain patterns in this paper as they can be observed microscopically in mono- and polycrystalline multilayers, and we will concentrate on the microscopic techniques to analyze them. It will become evident that in addition to the well known Kerr effect also the rarely applied magneto-optical Voigt and gradient effects have to be considered for a thorough and elegant domain analysis.

All images shown have been obtained by digitally enhanced magneto-optical (wide-field) microscopy [8] on the free surface of trilayer sandwiches with wedge-shaped spacer layers. Such wedge samples proved very favourable for microscopy [2] because they allow the direct comparison of the domains for the different types of coupling on the same specimen.

2. Domain overview

2.1. Epitaxial samples

Typical domain patterns for monocrystalline, epitaxially grown sandwiches are shown in Fig. 1. They have been observed by Kerr microscopy on an Fe/Cr/Fe wedge sample in the demagnetized state. The crystallographic orientation is such that two [100] easy axes of magnetization are running parallel to the film planes. Depending on the interlayer thickness we find different types of coupling in the same image, all of them showing their typical domain patterns.

The 90° and 180° domain walls observed for *ferromagnetic coupling* follow the principle of flux continuity so that net magnetic charges on the walls are avoided as far as possible (the normal components of magnetization on both sides of a wall have to be the same). Consequently, 90° walls are aligned at 45° relative to the easy axes and the 180° walls are oriented along the axes. Compared with the F-domains, the domains observed for *antiferromagnetic coupling* look rather irregular. The reason is obvious: since the magnetization vectors in both Fe layers are aligned anti-parallel, they cancel each other locally and

* Fax: +49-351 4659 541; e-mail: schaefer@ifw-dresden.d400.dc.

SSDI 0304-8853(95)00218-9

there is no net magnetization which would enforce a specific orientation of the domain walls. Often the irregular domains have a patch-like character (see Ref. [2]). For *biquadratic coupling* the magnetization vectors are aligned at 90° in both Fe layers. There are eight possibilities of doing so in a biaxial material. Two at a time, where the vectors in the top and bottom layers are exchanged, result in the same net magnetization which points along a diagonal 'hard' direction. Since the net magnetization is the same for two corresponding subphases, the orientations of the walls separating them may be arbitrary, while the net phase walls have to follow the rules of flux continuity. So the coexistence of regular and irregular domain walls is characteristic of biquadratic coupling.

2.2. *Sputtered samples*

Representative domain patterns for sputtered, polycrystalline sandwiches with an induced uniaxial anisotropy are collected in Fig. 2. For *ferromagnetic* coupling we find 180° domains (a) with walls running essentially along the easy axis. The transversely oriented lines are 360° walls [9] which show a characteristic double contrast when observed with a magneto-optical sensitivity perpendicular to the easy axis (a'). With the same setting also the strong ripple-modulation of the domain magnetization due to the polycrystalline nature of the material becomes visible.

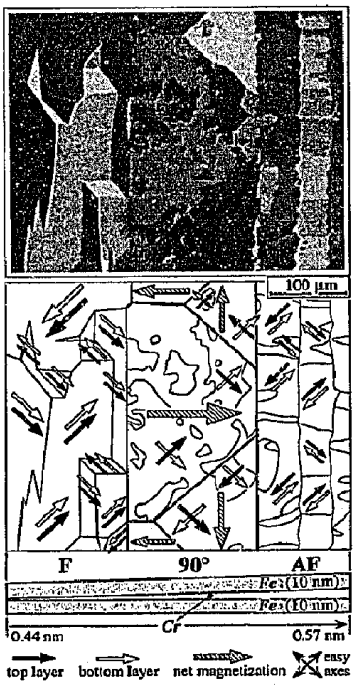

Fig. 1. Domains around the first transition region from ferro- to antiferromagnetic coupling on a monocrystalline Fe(10)/Cr(0.44–0.57)/Fe(10 nm) wedge sandwich (sample courtesy of P. Grünberg).

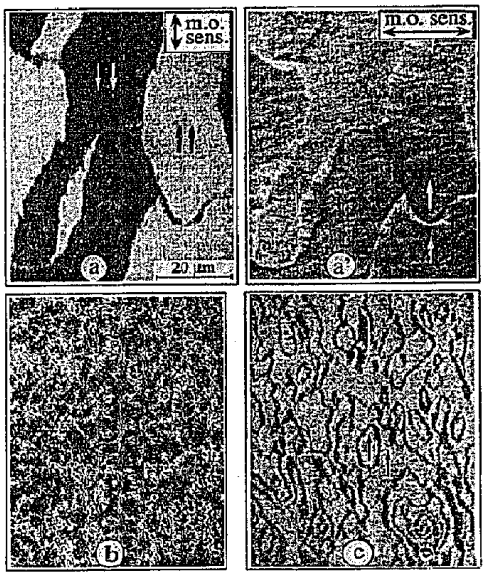

Fig. 2. Domains in F (a, a') and AF coupled (b) areas of a sputtered NiFe(3)/Ru/NiCo(3 nm) wedge sample. Images (a) and (a') show identical domain patterns, observed in the longitudinal Kerr effect at orthogonal planes of incidence. Image (c) was observed on NiCo(3)/Ru(3.7)/NiFe(3 nm)/MnFe (samples courtesy of S. Parkin).

Antiferromagnetically coupled films (b) are characterized by patch domains, similar to those found at nucleation in epitaxial sandwiches [2]. Finally, the case of *weakly coupled* ferromagnetic films as they occur for larger interlayer thicknesses or at a spacer thickness where the first-order coupling just changes sign from ferro- to antiferromagnetic. Here an accumulation of 360° walls is observed (c). In Ref. [5] we found that it requires quite high fields (some 100 Oe) to get rid of these walls, and that they act as nucleation sites in the magnetization process, making this process very irregular and irreversible.

3. Magneto-optical effects

The images in Figs. 1 and 2 have been obtained by means of the *Kerr* effect, the most widely applied magneto-optical effect for domain observation in reflection. In Ref. [10] two other effects detectable in reflection by digitally enhanced microscopy were discovered: the linear magnetic birefringence (called the *Voigt* or Cotton–Mouton effect) which is well known from transmission domain observations in garnets, and the *gradient* effect. All three effects are helpful for the domain analysis in multilayers, as will be elaborated later. Common to all is the generation of a magnetization-dependent magneto-optical light amplitude by illumination with plane polarized light. Under proper conditions, this amplitude is polarized at a right angle to the regularly reflected light and so can be detected

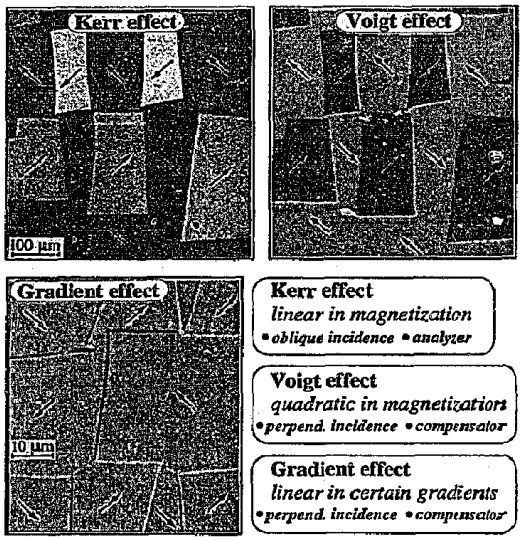

Fig. 3. Domains on an Fe(10)/Cr(0.3)/Fe(10 nm) sandwich, imaged in the Kerr, Voigt and gradient effects. The Kerr and Voigt images show identical domain patterns.

and converted into an observable contrast by an analyzer which largely blocks the regular light.

The phenomenological differences between the effects are compared in Fig. 3 together with some hints on the experimental conditions. The Kerr effect is a rotation effect and it is *linear* in magnetization. So the four domain phases in Fig. 3 show up in different colors. The same pattern imaged in the Voigt effect displays only two colors, one for each magnetization axis. This contrast is independent of the magnetization direction since the Voigt effect is a *quadratic* effect. The gradient effect is sensitive to changes in magnetization, which is why domain boundaries show up in this effect with a contrast depending on the magnetization direction of the domains. Both the Voigt and gradient effects are strongest at perpendicular incidence and they require a compensator (e.g. a quarter-wave plate) because their magneto-optical amplitude is shifted in phase relative to the regular amplitude.

4. Depth-selective domain observations

In magneto-optic microscopy of metals the magnetic information depth may be assumed to be at least 20 nm. This means for multilayers, that in addition to the (stronger) contrast of the top layer we will also get a contrast from lower layers if the upper layer is thinner than the mentioned thickness.

A quantification of the depth sensitivity was given by Träger et al. [11]. They found that the magneto-optical amplitude which is generated at a certain depth is a complex number and has an exponential depth dependence. So the amplitude is more and more damped the deeper in the material it is generated and it is shifted in its phase relative to the amplitude produced right at the surface. In a magneto-optical experiment, a contrast is generated by interference of the regularly reflected light amplitude N and the magneto-optical (e.g. Kerr) amplitude K (see inset in Fig. 4). However, only light components which are in phase can interfere and generate a detectable plane-polarized wave. In the case of a phase shift we would have to add a rotatable compensator in order to shift the phases of N and K properly. The phase can be selected in such a way that the magnetization at the surface is detected optimally, meaning that N is allowed to interfere with the K generated right at the surface. By selecting another phase angle, a focus on subsurface magnetization components becomes possible.

The sensitivity curves in Fig. 4 show two possible choices in a magnetic sandwich. In each case the phase was selected so that the zero of the information depth is somewhere in the middle of one of the films. Then the integral contrast of this layer will vanish and only a Kerr component of the other layer will become visible. In other words, by proper phase selection we can image the magnetization of both layers separately.

A first experimental verification of this concept was made by Rührig [7]. Fig. 5 shows another example, observed on an FeCrFe wedge, where the three types of coupling coexist in one image. The Kerr contrast was carefully adjusted so that domains magnetized to the right and left are equally grey, while up and down domains are white and black, respectively. In the upper image the compensator was rotated in such a way that only the magnetization of the top Fe layer becomes visible, while in the lower image only the bottom layer shows up. In the regime of ferromagnetic coupling, identical domains have the same color in both layers (parallel magnetization), while for AF coupling the contrast is inverted. Of course the intensity of the bottom layer is lower than that of the top layer due to absorption. In the regime of biquadratic coupling, all domains imaged in white or black in the upper layer are grey in the bottom layer, and vice versa.

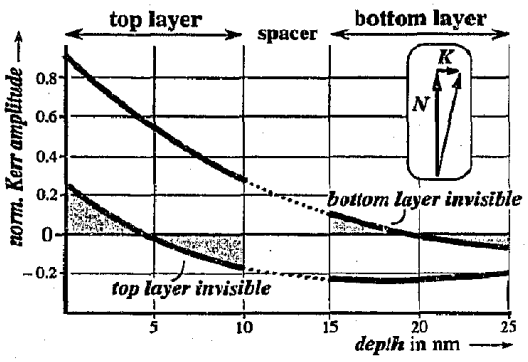

Fig. 4. Kerr amplitude in an Fe sandwich as a function of depth, schematically shown for two different compensator settings (courtesy of L. Wenzel)

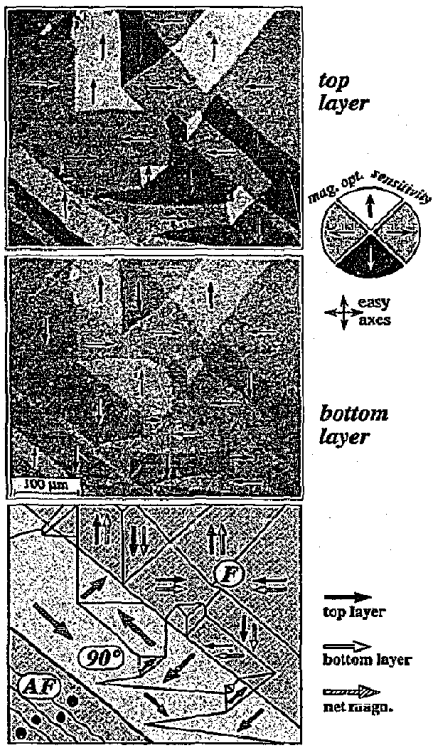

Fig. 5. Kerr contrast in an Fe(10)/Cr(~ 0.5)/Fe(10 nm) sandwich, observed separately in the two iron layers by proper phase selection with a phase shifting compensator.

Thus the 90° alignment of the magnetization vectors can be nicely confirmed by depth-selective experiments.

5. Voigt and gradient microscopy

In the general case, however, when we are not so careful with the adjustment of the compensator, the depth sensitivity of magneto-optic information can make the interpretation of Kerr contrasts rather difficult. Only in cubic trilayers can one expect up to 16 levels of grey when all types of coupling are considered. Some of them are visible in Fig. 1.

In such confusing situations, *Voigt microscopy* [6] offers an elegant alternative to the conventional Kerr effect, again by considering its depth sensitivity. An example is shown in Fig. 6, where the same domain pattern as in Fig. 1 is imaged in the Voigt effect. We find a strong black/white contrast in the F and AF areas, and a weaker two-level grey contrast in the biquadratic zone. The sketch helps to interpret those contrasts under consideration of the partial contributions from the two iron layers. The sensitivity function was adjusted so that the top layer contribution to the Voigt effect is stronger, but there is still some contrast also from the bottom layer. For F and AF coupling there are four possible magnetization arrangements in each case, two of them with the magnetization along the black 'Voigt axis' and the other two along the white axis. Since the sign of the (quadratic) Voigt contrast is the same in both iron layers it adds up to a strong black and white contrast. In the 90° zone there are eight possible magnetization arrangements. In four of them the top layer is magnetized along the black axis, but this black is weakened by the opposed Voigt contrast from the bottom layer. Correspondingly, the white from the top layer is darkened by the orthogonally magnetized bottom layer for the other four possibilities. So we end up with a weak black/white contrast in the 90° zone and a strong black and white Voigt contrast in the F and AF regions. Obviously the three different areas of coupling can very easily be distinguished in the Voigt image, much easier than in the multicontrast Kerr image of Fig. 1.

This knowledge can now be applied to more complicated domain patterns like those in Figs. 7 and 8. Again the Voigt contrast immediately tells us how to interpret them. The domains in Fig. 7 show four Voigt grey levels. From the previous discussion we know that black and white indicates collinear (parallel or antiparallel) alignment, while weak and strong grey indicates 90° alignment. Since all four colors coexist and are mixed together and because the colors can be arranged differently by applying an external field, we can conclude that this must be uncoupled behavior, or more precisely, a behavior where a weak coupling is dominated by coercivity effects. It is hard to distinguish uncoupled from F-coupled layers in hysteresis measurements. In Voigt microscopy, however, this is immediately possible.

The domains in Fig. 8 were observed on an iron sandwich where the nonmagnetic interlayer was a trilayer itself with silver embedded in chromium. This material tends to 90° coupling, but sometimes around material

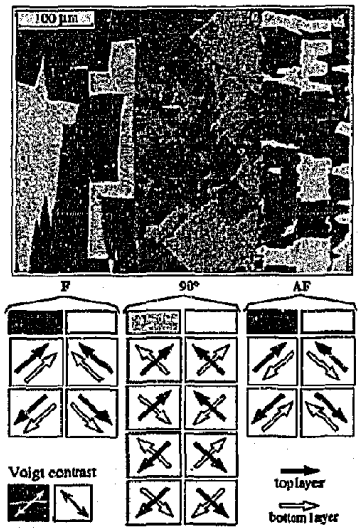

Fig. 6. Voigt contrast on the same domain pattern as in Fig. 1, together with a schematic explanation.

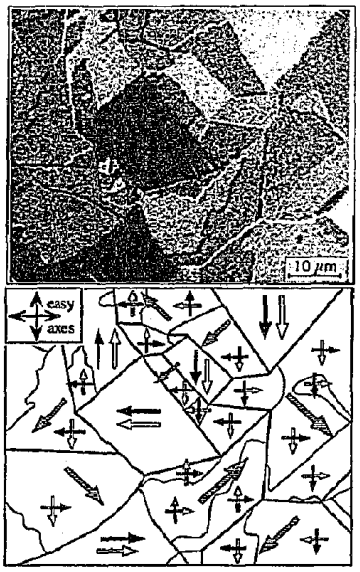

Fig. 7. Imaging at perpendicular incidence: Voigt and gradient contrast on an Fe(10)/Al(2.2)/Fe(10 nm) sandwich (sample courtesy of A. Fuss and P. Grünberg).

defects there are locations (like in the center of the images in Fig. 8) where this is not true. While an interpretation of the Kerr image (Fig. 8a) seems rather complicated, the domains can easily be unraveled in Voigt microscopy (Fig. 8b): the Voigt image shows a patch of strong contrast with regular domain walls, imbedded in a low-contrast matrix.

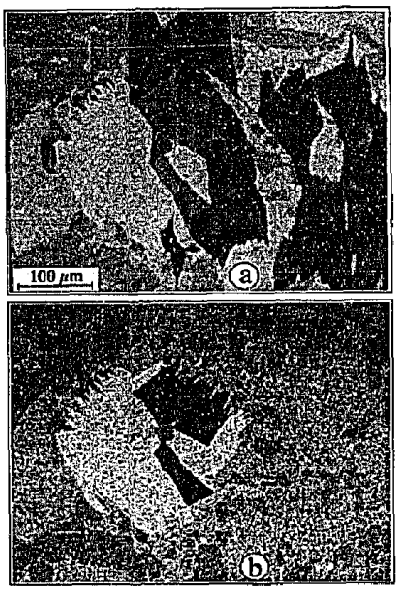

Fig. 8. Kerr (a) and Voigt (b) contrast on identical domains, observed on an Fe(5)/Cr(0.8)–Ag(0.4)–Cr(0.8)/Fe(5 nm) sandwich. A region of ferromagnetic coupling around a defect (strong Voigt contrast) is embedded in an otherwise 90°-coupled environment (sample courtesy V. Cros and P. Grünberg).

So there is obviously some ferromagnetic coupling around the defect in an otherwise biquadratically coupled environment.

Moreover, a domain model like in Fig. 7 can easily be constructed by just studying the contrasts in the image which in addition to the Voigt contrast also reveals the gradient contrast at the domain boundaries. To do this we first decide from the intensity of the Voigt contrast whether the vectors are aligned collinearly or orthogonally. Then we determine the axes of magnetization from the Voigt color (according to the sketch in Fig. 6, under the assumption of a stronger contribution of the top layer). Finally, the gradient contrast can be analyzed. It is determined by the orientation of a domain boundary, together with the orientation of the magnetization difference vector (net difference vector in the case of biquadratic coupling) of its neighboring domains, both relative to the given polarization axis of light [10]. So a definite determination of the direction of the domain magnetization vectors becomes possible. For a detailed example of such an analysis on multilayers, see Ref. [7]. In constructing a magnetization map one should of course never forget the rules of micromagnetics, that is, the orientation of the domain walls. Only if a model is fully compatible with both the wall orientations and the contrasts, can we be sure about it.

6. Conclusions

Magneto-optical microscopy with its depth sensitivity of contrast offers the potential to analyze the domain patterns in coupled magnetic multilayers. In biaxial materials, microscopy at perpendicular incidence, that is Voigt and gradient microscopy, can be an attractive method in addition to Kerr microscopy. It requires, however, an image processor since the Voigt and gradient effects usually are weaker than the Kerr effect.

Acknowledgements: Most of the imaging has been done at Erlangen University, and I very much appreciate collaboration with Alex Hubert, Manfred Rührig, J. McCord and L. Wenzel. The work on sputtered materials was started in Bernie Argyle's group in Yorktown Heights in collaboration with P. Trouilloud. Thanks also to the suppliers of excellent samples: W. Zinn, P. Grünberg, R. Schreiber, M. Schäfer, M. Schneider, Q. Leng, V. Cros, A. Wolf and A. Fuss, (all KFA Jülich), and S. Parkin and V. Speriosu (IBM Almaden).

References

[1] P. Grünberg, R. Schreiber, Y. Pang, M.B. Brodsky and H. Sowers, Phys. Rev. Lett. 57 (1986) 2442; S.S.P. Parkin, N. More and K.P. Roche, Phys. Rev. Lett. 64 (1990) 2304; J. Unguris, R.J. Celotta and D.T. Pierce, Phys. Rev. Lett. 67 (1991) 140.

[2] M. Rührig, R. Schäfer, A. Hubert, R. Mosler, J.A. Wolf, S. Demokritov and P. Grünberg, Phys. Stat. Solid (a) 125 (1991) 635.
[3] C. Chen, Y. Idzerda, H.-J. Lin, G. Meigs, A. Chaiken, G. Prinz and G. Ho, Phys. Rev. B 48 (1993) 1; or see Y. Idzerda, 14th Int. Coll. Magn. Films Surfaces, Conf. Abstracts Paper E1, Düsseldorf 1994.
[4] See, e.g., J. McCord, H. Brendel and A. Hubert, 14th Int. Coll. Magn. Films Surfaces, Conf. Abstracts Paper D78, Düsseldorf 1994; R. Kergoat, J. Miltat, P.P Freitas and J.L. Leal, 14th Int. Coll. Magn. Films Surfaces, Conf. Abstracts Paper D89, Düsseldorf 1994.
[5] R. Schäfer, A. Hubert and S.S.P. Parkin, IEEE Trans. Magn. 29 (1993) 2738.
[6] J. McCord, A. Hubert, R. Schäfer, A. Fuß and P. Grünberg, IEEE Trans. Magn. 29 (1993) 2735.
[7] M. Rührig, dissertation, University of Erlangen (1993).
[8] F. Schmidt, W. Rave and A. Hubert, IEEE Trans. Magn. 21 (1985) 1596.
[9] E. Sannek, M. Rührig and A. Hubert, IEEE Trans. Magn. 29 (1993) 2500.
[10] R. Schäfer and A. Hubert, Phys. Stat. Solidi (a) 118 (1990) 271.
[11] G. Träger, L. Wenzel and A. Hubert, Phys. Stat. Solidi (a) 131 (1992) 201; A. Hubert and G. Träger, J. Magn. Magn. Matet. 124 (1993) 185.